

UC San Diego

UC San Diego Previously Published Works

Title

Viral Determinants in H5N1 Influenza A Virus Enable Productive Infection of HeLa Cells.

Permalink

<https://escholarship.org/uc/item/0106p40s>

Journal

Journal of Virology, 94(4)

Authors

Rodriguez-Frandsen, Ariel

Martin-Sancho, Laura

Gounder, Anshu

et al.

Publication Date

2020-01-31


DOI

10.1128/JVI.01410-19

Peer reviewed



Viral Determinants in H5N1 Influenza A Virus Enable Productive Infection of HeLa Cells

Ariel Rodriguez-Frandsen,^a Laura Martin-Sancho,^a Anshu P. Gounder,^a Max W. Chang,^b Wen-Chun Liu,^{c,d} Paul D. De Jesus,^a Jessica von Recum-Knepper,^a Miriam S. Dutra,^a Nicholas J. Huffmaster,^a Monica Chavarria,^a Ignacio Mena,^{c,d} Laura Riva,^a Courtney B. Nguyen,^a Saunil Dobariya,^a Kristina M. Herbert,^a Christopher Benner,^b  Randy A. Albrecht,^{c,d} Adolfo García-Sastre,^{c,d,e,f} Sumit K. Chanda^a

^aInfectious and Inflammatory Diseases Center, Sanford Burnham Prebys Medical Discovery Institute, La Jolla, California, USA

^bDepartment of Medicine, University of California, San Diego, California, USA

^cDepartment of Microbiology, Icahn School of Medicine at Mount Sinai, New York, New York, USA

^dGlobal Health and Emerging Pathogens Institute, Icahn School of Medicine at Mount Sinai, New York, New York, USA

^eDepartment of Medicine, Division of Infectious Diseases, Icahn School of Medicine at Mount Sinai, New York, New York, USA

^fThe Tisch Cancer Institute, Icahn School of Medicine at Mount Sinai, New York, New York, USA

Ariel Rodriguez-Frandsen, Laura Martin-Sancho, and Anshu P. Gounder contributed equally to this work.

ABSTRACT Influenza A virus (IAV) is a human respiratory pathogen that causes yearly global epidemics, as well as sporadic pandemics due to human adaptation of pathogenic strains. Efficient replication of IAV in different species is, in part, dictated by its ability to exploit the genetic environment of the host cell. To investigate IAV tropism in human cells, we evaluated the replication of IAV strains in a diverse subset of epithelial cell lines. HeLa cells were refractory to the growth of human H1N1 and H3N2 viruses and low-pathogenic avian influenza (LPAI) viruses. Interestingly, a human isolate of the highly pathogenic avian influenza (HPAI) H5N1 virus successfully propagated in HeLa cells to levels comparable to those in a human lung cell line. Heterokaryon cells generated by fusion of HeLa and permissive cells supported H1N1 virus growth, suggesting the absence of a host factor(s) required for the replication of H1N1, but not H5N1, viruses in HeLa cells. The absence of this factor(s) was mapped to reduced nuclear import, replication, and translation, as well as deficient viral budding. Using reassortant H1N1:H5N1 viruses, we found that the combined introduction of nucleoprotein (NP) and hemagglutinin (HA) from an H5N1 virus was necessary and sufficient to enable H1N1 virus growth. Overall, this study suggests that the absence of one or more cellular factors in HeLa cells results in abortive replication of H1N1, H3N2, and LPAI viruses, which can be circumvented upon the introduction of H5N1 virus NP and HA. Further understanding of the molecular basis of this restriction will provide important insights into the virus-host interactions that underlie IAV pathogenesis and tropism.

IMPORTANCE Many zoonotic avian influenza A viruses have successfully crossed the species barrier and caused mild to life-threatening disease in humans. While human-to-human transmission is limited, there is a risk that these zoonotic viruses may acquire adaptive mutations enabling them to propagate efficiently and cause devastating human pandemics. Therefore, it is important to identify viral determinants that provide these viruses with a replicative advantage in human cells. Here, we tested the growth of influenza A virus in a subset of human cell lines and found that abortive replication of H1N1 viruses in HeLa cells can be circumvented upon the introduction of H5N1 virus HA and NP. Overall, this work leverages the genetic diversity of multiple human cell lines to highlight viral determinants that could contribute to H5N1 virus pathogenesis and tropism.

Citation Rodriguez-Frandsen A, Martin-Sancho L, Gounder AP, Chang MW, Liu W-C, De Jesus PD, von Recum-Knepper J, Dutra MS, Huffmaster NJ, Chavarria M, Mena I, Riva L, Nguyen CB, Dobariya S, Herbert KM, Benner C, Albrecht RA, García-Sastre A, Chanda SK. 2020. Viral determinants in H5N1 influenza A virus enable productive infection of HeLa cells. *J Virol* 94:e01410-19. <https://doi.org/10.1128/JVI.01410-19>.

Editor Stacey Schultz-Cherry, St. Jude Children's Research Hospital

Copyright © 2020 American Society for Microbiology. All Rights Reserved.

Address correspondence to Sumit K. Chanda, schanda@sbpdiscovery.org.

Received 20 August 2019

Accepted 4 November 2019

Accepted manuscript posted online 27 November 2019

Published 31 January 2020

KEYWORDS H5N1, HeLa, heterokaryon, highly pathogenic, influenza A virus

Influenza A viruses (IAVs) are important human respiratory pathogens responsible for yearly epidemics that cause approximately 250,000 to 500,000 fatalities worldwide (1–3). While most IAV strains are restricted to their natural reservoir, aquatic birds, certain IAVs can adapt to new host species and produce novel pathogenic strains with pandemic potential (4). Over the last century and as recently as the beginning of the 21st century, four influenza pandemics have occurred in the human population: the 1918 H1N1 Spanish flu, the 1957 H2N2 Asian flu, the 1968 H3N2 Hong Kong flu, and the 2009 H1N1 swine flu pandemic. In addition, sporadic zoonotic transmission of avian viruses of subtypes H5, H6, H7, H9, and H10 has been detected in humans (5). Of these, highly pathogenic avian influenza (HPAI) H5N1 viruses have caused >860 confirmed human infections in 17 countries, with a 52% mortality rate, and pose a significant threat to global health (6). While circulating H5N1 viruses cause limited human-to-human transmission, repeated zoonotic outbreaks might provide the basis for efficient propagation and spread—an event that may require <5 mutations (7, 8). Therefore, it is critical to gain a better understanding of the viral and host factors required for H5N1 viruses to replicate efficiently and to be transmitted to a broader host range.

IAV is an enveloped RNA virus with a segmented negative-sense genome that hijacks the host cell machinery for replication. For productive infection, IAV needs to (i) attach to and enter the host cell, (ii) replicate and transcribe its viral genome and translate it into viral proteins, and (iii) traffic, assemble, and release progeny virions to infect neighboring cells (9, 10). Global loss-of-function screens have identified multiple host factors required for IAV replication (11–15). Differences in the expression levels of these factors across cell types dictate the ability of IAV to infect and complete its infectious cycle. The multitude of available cell lines from diverse human tissues can provide an experimental system for the discovery of host dependency factors and host restriction factors (16–21), or the identification of viral determinants (22–25), by comparison of cells that are permissive or restrictive for viral growth. Viral determinants that increase IAV replication and pathogenesis have been described previously (23, 26). An example is the cleavage of the surface protein hemagglutinin (HA). The cleavage site of HA proteins from low-pathogenic avian influenza (LPAI) viruses contains a single basic residue that can be cleaved only by cellular proteases found on mucosal surfaces. However, HA proteins from HPAI viruses, such as H5N1 viruses, contain a polybasic cleavage site that can be cleaved by ubiquitous furin-like proteases, extending the tissue tropism of these viruses and facilitating systemic infection (27, 28). In addition, several amino acids in the viral polymerases (PA, PB1, and PB2), NP, and NS1 have been associated with increased pathogenicity of HPAI viruses in mammals (29, 30). Identifying and understanding these host- and strain-specific determinants can provide insights into virulence, cellular tropism, and host range—factors that are crucial for assessing the pandemic potential of IAVs.

Here, we evaluated the ability of influenza virus to replicate and spread in a varied subset of human epithelial cell lines. Interestingly, several human H1N1, H3N2, and LPAI strains were unable to grow in HeLa cells, but we observed efficient propagation of a human isolate of an H5N1 virus with a modified HA cleavage site. Heterokaryon cells, produced by fusion of HeLa and permissive 293T cells, supported H1N1 virus growth, suggesting that H1N1 virus restriction in HeLa cells is the consequence of the absence or low expression of a host factor(s) essential for the replication of H1N1 viruses but not H5N1 viruses. Entry of H1N1 viruses into HeLa cells was unaffected, but we found reduced nuclear import, viral replication, and translation, as well as defective virus budding. The introduction of H5N1 virus NP and HA enabled productive replication of H1N1 virus in HeLa cells, suggesting that these factors are necessary to circumvent the replicative defect in HeLa cells.

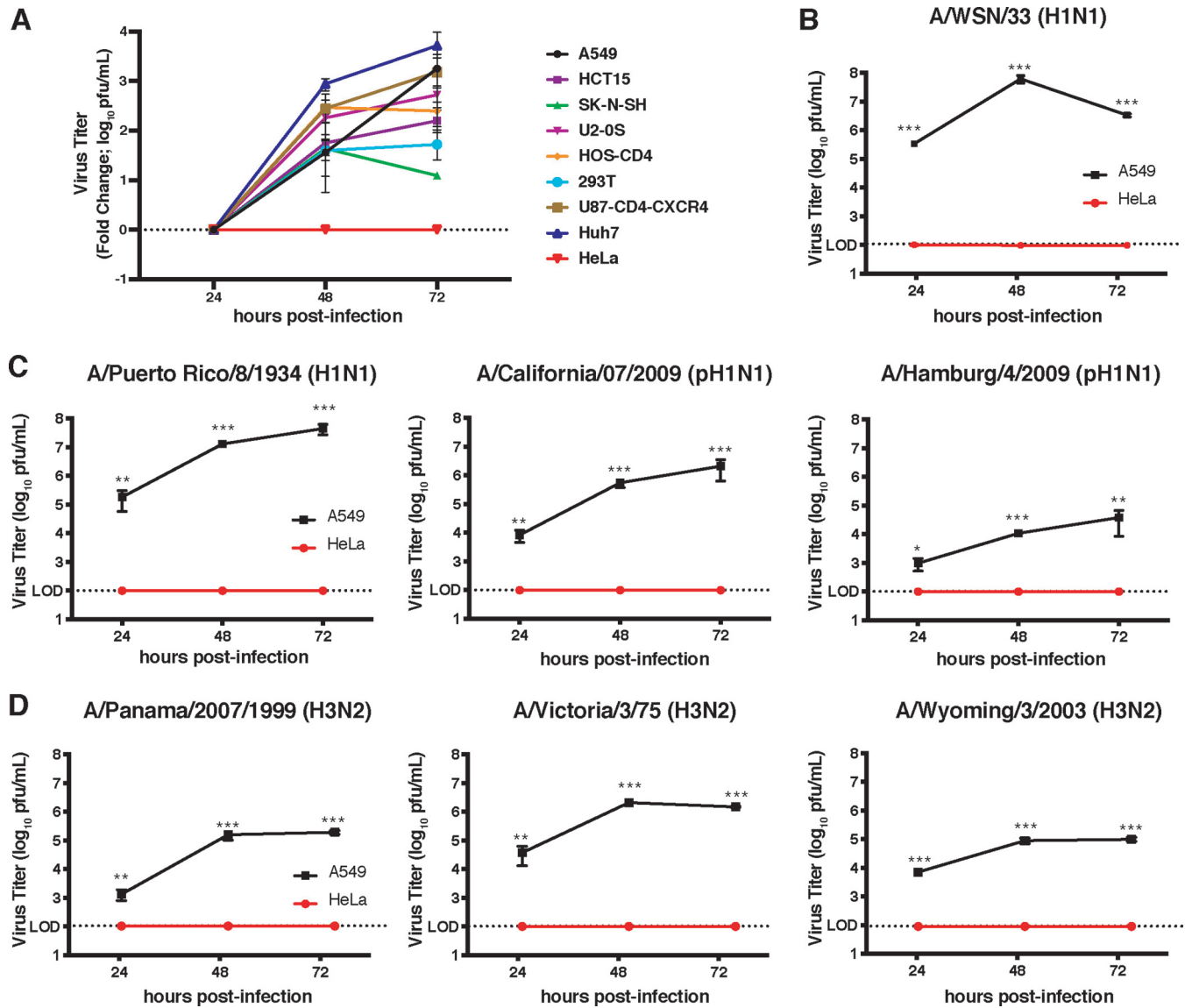


FIG 1 HeLa cells do not support H1N1 or H3N2 IAV growth. (A) Nine epithelial cell lines (A549, HCT15, SK-N-SH, U2OS, HOS-CD4, HEK293T, U87-CD4-CXCR4, Huh-7, and HeLa cells) were infected with IAV A/WSN/33 at an MOI of 0.01. At the indicated hours postinfection, cell culture supernatants were collected, and the amount of infectious virus released was measured by a plaque assay. Plotted is the fold change in titer from 24 hpi for each cell line. Data are averages from two independent biological experiments. The limit of detection (LOD) for the plaque assay is indicated by a dotted black line at 1×10^2 PFU/ml. (B through D) Infectious virus titers in supernatants from A549 (solid black lines) or HeLa (solid red lines) cells infected with A/WSN/33 (B) or the indicated H1N1 (C) or H3N2 (D) IAV strains at an MOI of 0.01. Data are averages from three independent biological experiments and represent mean \pm standard deviation. Asterisks indicate significant differences by multiple Student *t* tests (*, $P \leq 0.05$; **, $P \leq 0.001$; ***, $P \leq 0.0001$).

RESULTS

Differential susceptibility of human epithelial cell lines to influenza A virus growth. Nine human epithelial cell lines, A549, HCT15, SK-N-SH, U2-OS, HOS-CD4, HEK293T, U87-CD4-CXCR4, Huh-7, and HeLa cells, were systematically compared for their abilities to support multicycle replication of human influenza virus A/WSN/33 (H1N1). These cell lines were infected at a low multiplicity of infection (MOI) (0.01 PFU/cell), and infectious virus titers in the supernatants were measured at 24, 48, and 72 h postinfection (hpi). We observed that while eight of the nine cell lines supported productive A/WSN/33 infection, as shown by increases in virus titers over time, no viral growth was detected in HeLa cells (Fig. 1A). Abortive replication of IAVs in HeLa cells has already been described (31–35). However, those studies were limited to a small subset of IAV strains, and the mechanism was not fully elucidated. Therefore, we sought

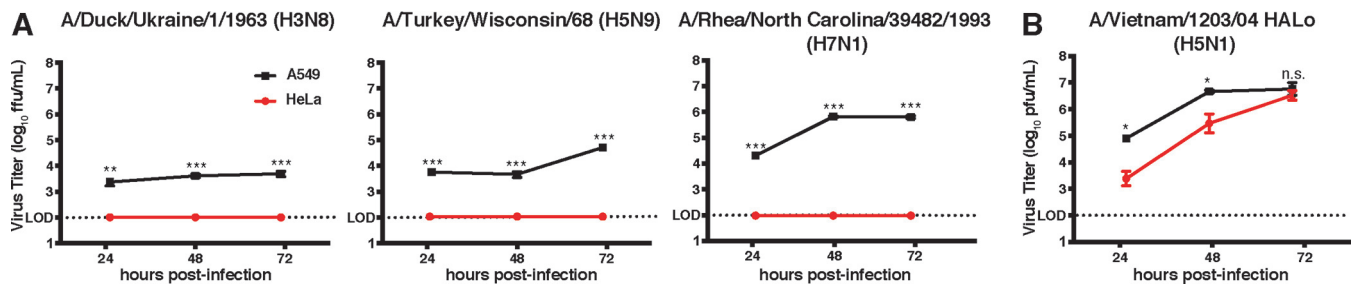


FIG 2 HeLa cells support the replication of a highly pathogenic avian IAV (H5N1) strain. A549 (solid black lines) or HeLa (solid red lines) cells were infected with the indicated LPAI strains (A) or H5N1-HaLo (B) at an MOI of 0.01, and infectious virus titers in the cell culture supernatants were measured at 24, 48, and 72 hpi via a focus-forming assay (with results expressed in focus-forming units [FFU] per milliliter) (A) or a plaque assay (with results expressed in PFU per milliliter) (B). Data are averages from three independent biological experiments and represent mean \pm standard deviation. The limits of detection (LOD) for the focus-forming assay and plaque assay are indicated by dotted black lines at 1×10^2 PFU/ml. Asterisks indicate significant differences by multiple Student *t* tests (*, $P \leq 0.05$; **, $P \leq 0.001$; ***, $P \leq 0.0001$).

to conduct a more comprehensive assessment of this phenotype. Since the A549 human lung epithelial cell line was permissive for productive A/WSN/33 infection and is a well-characterized model for IAV infection and growth, we chose A549 cells for subsequent experiments. Further analysis of infectious virus release following A/WSN/33 infection confirmed abortive infection in HeLa cells (titers, in PFU per milliliter, were less than or equal to the assay limit of detection [LOD] of 1×10^2 PFU/ml at 24, 48, and 72 hpi), in contrast to A549 cells (titers of 1.9×10^5 PFU/ml at 24 hpi, 2.6×10^7 PFU/ml at 48 hpi, and 1.7×10^6 PFU/ml at 72 hpi) ($P \leq 0.0001$) (Fig. 1B). To investigate the strain and serotype specificity of this phenotype, we tested the replication kinetics of other H1N1 (lab-adapted A/Puerto Rico/8/1934, pandemic A/California/07/2009, and pandemic A/Hamburg/4/2009) and H3N2 (A/Panama/2007/1999, A/Victoria/3/75, and A/Wyoming/3/2003) IAV strains. While A549 cells supported the growth of all strains (with titers of $\geq 1 \times 10^4$ PFU/ml at 72 hpi), no infectious viruses were detected from HeLa cells (titers, $\leq 1 \times 10^2$ PFU/ml at all time points) (Fig. 1C and D). Collectively, these data show that HeLa cells do not support productive infection of a subset of human H1N1 and H3N2 IAVs.

HeLa cells support multicycle replication of H5N1 influenza A virus but not of other avian LPAI strains. To test if species-specific differences in IAV strains affect growth in HeLa cells, we analyzed the abilities of several LPAI strains to replicate in HeLa and A549 cells. Influenza viruses A/Duck/Ukraine/1/1963 (H3N8), A/Turkey/Wisconsin/68 (H5N9), and A/Rhea/North Carolina/39482/1993 (H7N1) generated infectious particles in A549 cells with titers of 3.7×10^3 FFU/ml, 3.3×10^4 FFU/ml, and 4×10^5 FFU/ml at 72 hpi, respectively. However, we did not observe any released particles in HeLa cells ($\leq 1 \times 10^2$ FFU/ml) (Fig. 2A).

The HPAI H5N1 strain is responsible for several human outbreaks and is linked to increased virulence and pathogenesis (5). To investigate IAV H5N1 growth in HeLa cells, we selected an H5N1 isolate from a fatal human case that was engineered to allow biosafety level 2+ work through a deletion in the HA polybasic cleavage site, A/Vietnam/1203/2004 HALo (referred to below as H5N1-HaLo) (36). Surprisingly, HeLa cells supported productive infection by H5N1-HaLo, and by 72 hpi, virus release in HeLa cells was comparable to that in A549 cells (3.3×10^6 PFU/ml and 5.7×10^6 PFU/ml, respectively) ($P = 0.45$) (Fig. 2B). Taken together, these data show that HeLa cells are refractory to the growth of human H1N1, H3N2, and LPAI viruses but allow successful replication of H5N1-HaLo. Since all H1N1 and H3N2 IAVs tested showed similar growth phenotypes in HeLa cells and similar growth phenotypes in A549 cells, we chose influenza virus A/WSN/33 (H1N1) for subsequent experiments.

Abortive replication of several IAVs in HeLa cells is not due to expression of human papillomavirus proteins. Previous work has shown that HeLa cells harbor integrated human papillomavirus 18 (HPV18) DNA within their genomes (37–39). RNA sequencing (RNA-seq) analysis of HeLa cells, either uninfected or infected with

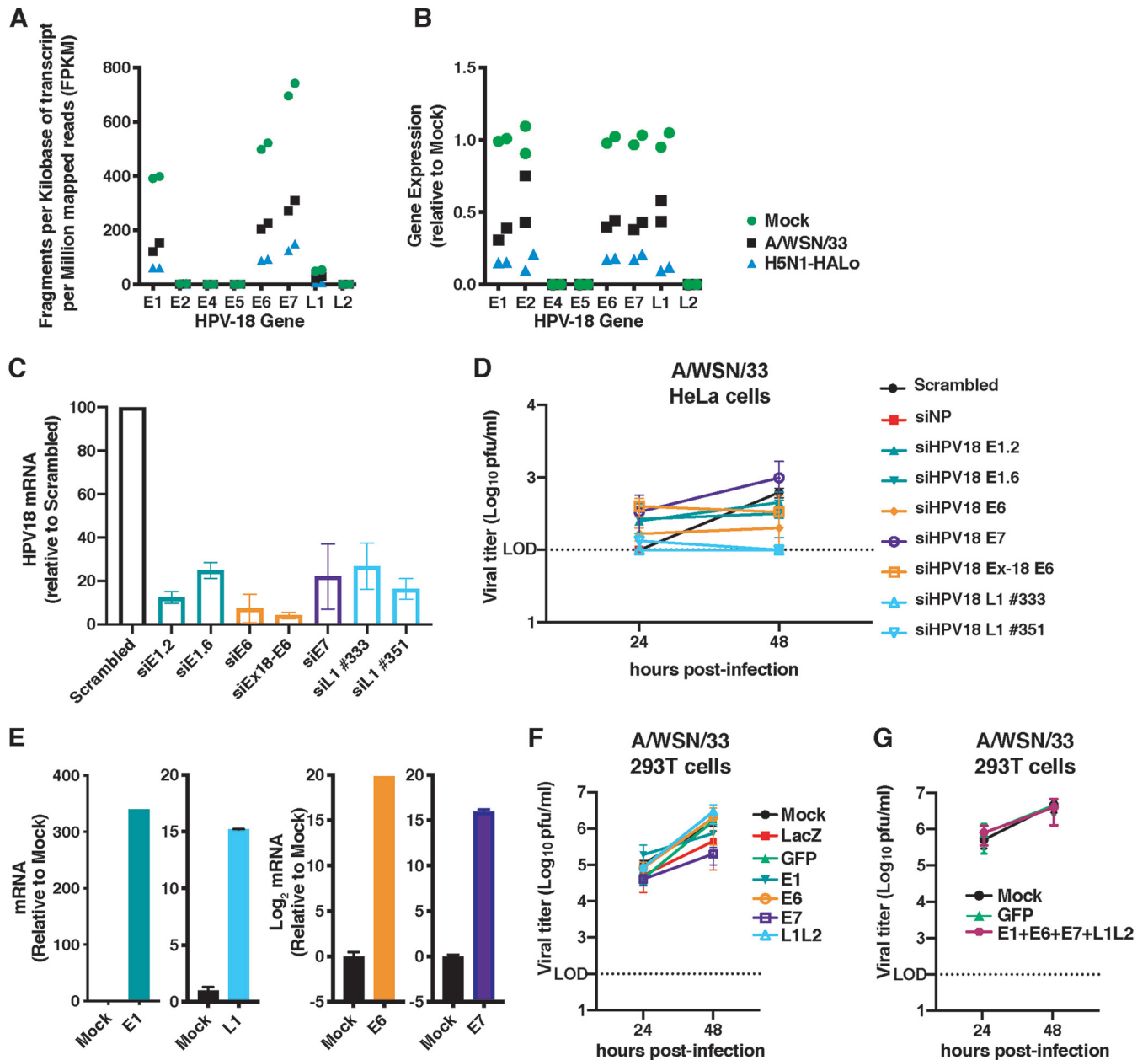


FIG 3 Abortive replication of several IAVs in HeLa cells is not due to the expression of human papillomavirus proteins. (A and B) HeLa cells were either mock infected or infected with A/WSN/33 or H5N1-HaLo at an MOI of 3. At 9 hpi, cell extracts were collected, and total RNA was isolated for RNA sequencing. The expression of each of the HPV18 genes is shown as the fragments per kilobase of transcript per million mapped reads (FPKM) (A) or as fold gene expression relative to that in mock-infected samples (B). (C) HeLa cells transfected with siRNAs targeting the indicated HPV18 genes or a negative-control siRNA (Scrambled). Knockdown efficiency at 48 h was determined by qRT-PCR. Values were normalized to that for TBP and were then graphed as the fold change relative to expression with the scrambled siRNA. (D) HeLa cells were transfected with the indicated siRNAs for 48 h and were then infected with A/WSN/33 at an MOI of 0.01. At the indicated times, the virus titer was determined by a plaque assay. (E) qRT-PCR validation of HPV gene overexpression in 293T cells. Values were normalized to that for TBP and were then graphed as the fold change relative to expression in mock-infected cells. (F and G) Cells overexpressing control genes, individual HPV18 genes (F), or a combination of HPV18 genes (G) were infected with A/WSN/33 at an MOI of 0.01, and at the indicated times, the virus titer was determined by a plaque assay. Data are mean \pm standard deviation from at least two independent experiments. The limit of detection (LOD) for the plaque assay is indicated by a dotted black line at 1×10^2 PFU/ml.

A/WSN/33 or H5N1-HaLo, confirmed mRNA expression of the HPV18 E1, E6, E7, and L1 genes (Fig. 3A and B). To evaluate if the expression of these genes could be responsible for the abortive replication of several IAV strains in HeLa cells, we successfully knocked down E1, E6, E7, and L1 using small interfering RNA (siRNA) (Fig. 3C) and measured the production of the A/WSN/33 virus at 24 and 48 hpi. No significant differences in viral

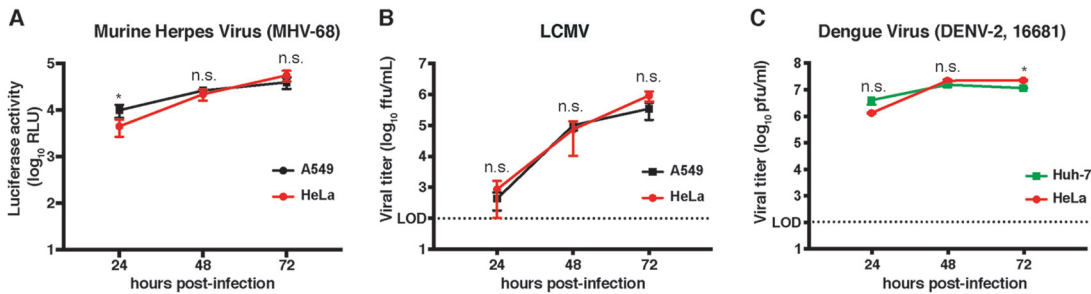


FIG 4 HeLa cells support productive infection by other RNA and DNA viruses. A549, Huh-7, or HeLa cells were infected with a murine gammaherpesvirus 68 (MHV-68) luciferase reporter virus (MOI, 0.1) (A), lymphocytic choriomeningitis virus (LCMV) (MOI, 0.01) (B), or dengue virus 16681 (DENV-2) (MOI, 10) (C). At the indicated times postinfection, luciferase activity was measured in cell lysates to assess MHV replication (A) or infectious virus titers were measured by a focus forming assay (B) or a plaque assay (C). Data are mean \pm standard deviation from at least two independent biological experiments. The limits of detection (LOD) for the focus-forming and plaque assay are indicated by dotted black lines at 1×10^2 PFU/ml. Asterisks indicate significant differences by multiple Student *t* tests (*, $P \leq 0.05$; **, $P \leq 0.001$; ***, $P \leq 0.0001$).

growth were found between siRNA-transfected HeLa cells and HeLa cells transfected with negative-control scrambled siRNA (Fig. 3D). Conversely, we overexpressed HPV18 E1, E6, E7, and L1 (Fig. 3E) in the IAV-permissive 293T cell line and found that neither individual (Fig. 3F) nor combined (Fig. 3G) expression of these viral genes reduced A/WSN/33 growth from that in cells expressing LacZ or green fluorescent protein (GFP). Collectively, these results indicate that the expression of HPV18 E1, E6, E7, and L1 genes is not responsible for defective IAV growth in HeLa cells.

HeLa cells support productive infection by other RNA and DNA viruses. We then tested if HeLa cells could support efficient replication of non-IAV viruses. Murine gammaherpesvirus 68 (MHV-68), lymphocytic choriomeningitis virus (LCMV), and dengue virus 16681 (DENV-2) were selected on the basis of their genome characteristics (RNA or DNA, segmented or nonsegmented, positive sense or negative sense) and site of replication (nuclear or cytoplasmic). Productive replication by all three viruses was detected in HeLa cells (Fig. 4A to C), suggesting that the inability of multiple IAV strains to propagate in HeLa cells is not due to a general defect in these cells.

Growth of human H1N1 IAV in HeLa cells is supported upon fusion with permissive 293T cells. Restriction in HeLa cells of a subset of IAVs that propagate efficiently in other cell types poses at least two possibilities: (i) HeLa cells might contain a factor(s) that impairs viral growth or (ii) permissive cells might contain a factor(s) that is required for productive viral replication, and this factor(s) might be deficient or expressed at low levels in HeLa cells. To investigate these possibilities, we induced the fusion of HeLa-mCherry and IAV-permissive 293T-zsGreen cells using vesicular stomatitis virus G protein (VSV-G) (40). HeLa-293T heterokaryons were selected based on sorting of mCherry-zsGreen double-positive cells with a fluorescence-activated cell sorter (FACS) (Fig. 5A and B) and were subsequently infected with A/WSN/33 or H5N1-HaLo. The growth of the A/WSN/33 virus was enhanced in HeLa-293T heterokaryons over that in HeLa-mCherry cells (Fig. 5C), suggesting the likely presence of a positive factor(s) in 293T cells that can support H1N1 virus growth in the heterokaryon cells (see Discussion). As expected, production of H5N1-HaLo infectious virus was detected in all three cell lines (Fig. 5D). The amount of virus released from HeLa-293T heterokaryon cells was lower than that from parental 293T-zsGreen cells following infection with A/WSN/33 or H5N1-HaLo. It is likely that the full extent of IAV replication is decreased in these artificial heterokaryon cells. Additionally, the presence of unfused, nonpermissive HeLa-mCherry cells in the sorted heterokaryon population likely contributes to the limited infectious virus production following A/WSN/33 infection.

To ensure that the virus output we were observing was not due to the 3.60 to 0.51% carryover of unfused 293T-zsGreen cells during cell sorting, we infected a mixed population of 4% 293T-zsGreen and 96% HeLa-mCherry cells. This cell mixture produced A/WSN/33 virus at significantly lower levels than HeLa-293T heterokaryons at 48

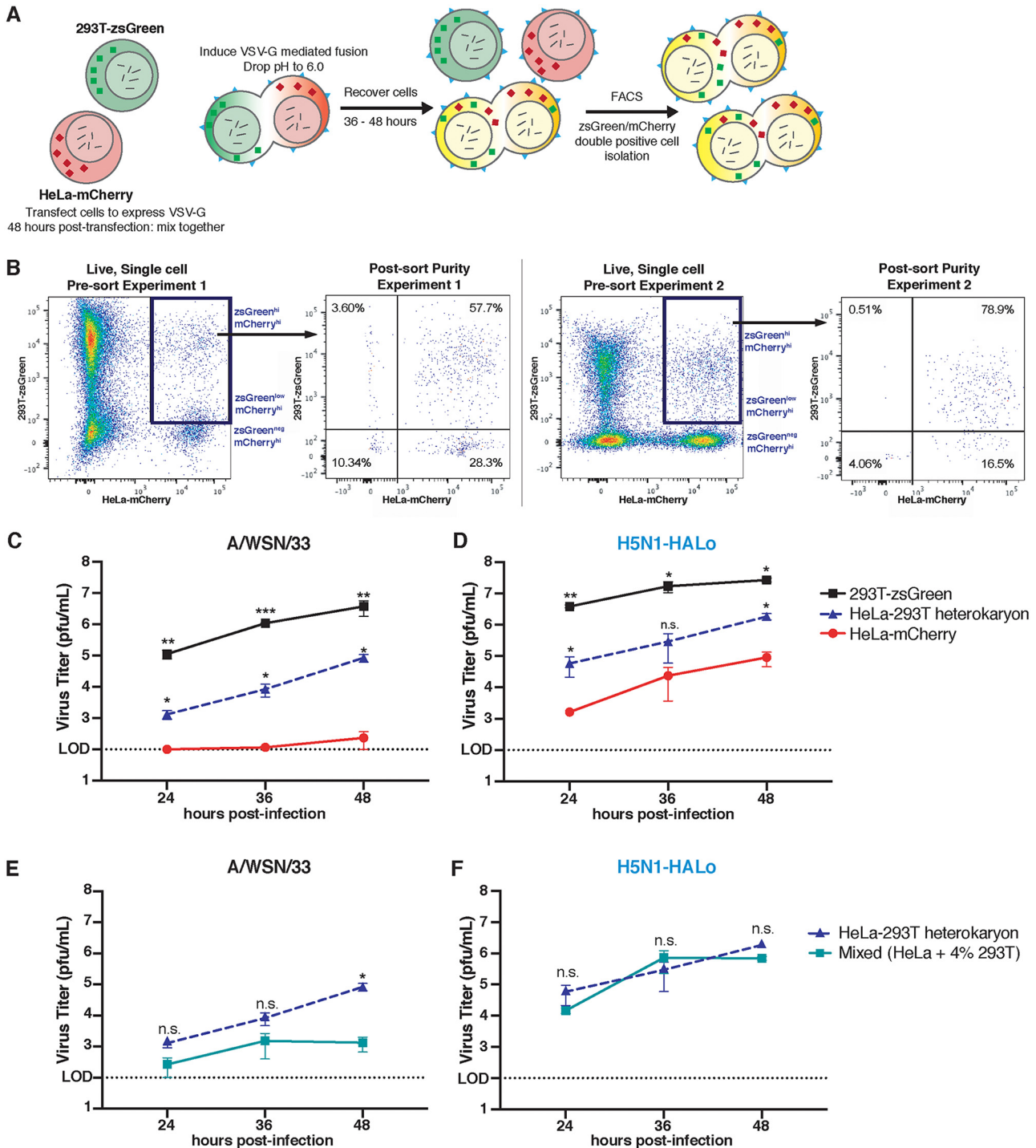


FIG 5 Growth of H1N1 virus in HeLa cells is supported upon fusion with permissive 293T cells. (A) Schematic for the production and isolation of HeLa-293T heterokaryons using HeLa-mCherry or 293T-zsGreen cells. Cells were transiently transfected with VSV-G and then exposed to a low pH in order to induce the fusogenic properties of VSV-G. Fused cells were FACS sorted for zsGreen-mCherry double-positive cells. (B) zsGreen^{hi} mCherry^{hi} and zsGreen^{low} mCherry^{hi} cell populations (presort; boxed area) were collected, and the purity of the sorted population was assessed (postsort purity) prior to downstream experiments. Pre- and postsort cell populations are shown for two independent experiments. Stringent gating criteria were used to exclude the collection of zsGreen single-positive cells. (C) HeLa-mCherry (solid red lines), 293T-zsGreen (solid black lines), or sorted HeLa-293T heterokaryons (dashed blue lines) were infected at an MOI of 0.01 with A/WSN/33 (C) or H5N1-HaLo (D). At the indicated times, cell culture supernatants were collected, and virus titers were determined by plaque assay. (E) Due to technical limitations, the cells collected included a small percentage ($\leq 4\%$) of live, single cells ($\leq 4\%$) of zsGreen single-positive cells (293T-zsGreen). A mixed population of 96% HeLa-mCherry cells and 4% 293T-zsGreen cells (solid cyan lines) was created and infected alongside sorted heterokaryons (HeLa-293T heterokaryons) (dashed blue lines) at an MOI of 0.01 with A/WSN/33 (E) or H5N1-HaLo (F). At the indicated times, virus titers were determined by plaque assay. Data points are mean \pm standard deviation from two independent biological experiments. The limit of detection (LOD) for the plaque assay is indicated by a dotted black line at 1×10^2 PFU/ml. Asterisks indicate significant differences (*, $P \leq 0.05$; **, $P \leq 0.001$; ***, $P \leq 0.0001$) for comparison to HeLa-mCherry by two-way analysis of variance (C and D) or multiple Student *t* tests (E and F).

hpi (Fig. 5E), despite similar growth of H5N1-HaLo (Fig. 5F). These data suggest that growth of the human H1N1 virus in HeLa cells can be detected upon fusion with a permissive cell line, indicating that HeLa cells are likely defective in one or more host factors that are essential for the replication of H1N1, but not H5N1, viruses.

HeLa cells show reduced nuclear import, replication, and translation, as well as deficient budding of H1N1 IAV. We next examined which step in the IAV infectious cycle was affected in HeLa cells by comparing the contrasting abilities of A/WSN/33 and H5N1-HaLo to replicate. Viral entry was investigated by measuring cytoplasmic NP following infection with A/WSN/33 or H5N1-HaLo in cells treated with cycloheximide (CHX), a general inhibitor of protein synthesis. NP intensity levels were comparable in the two strains, suggesting that viral entry was not affected (Fig. 6A). Nuclear import, measured by nuclear NP signal intensity, suggested a small, but statistically significant, reduction in the nuclear import of A/WSN/33 relative to that of H5N1-HaLo (mean nuclear NP signal intensities, 134 for A/WSN/33 and 180 for H5N1-HaLo [$P = 0.014$]) (Fig. 6B). Next, we evaluated the abilities of the A/WSN/33 and H5N1-HaLo viruses to drive a minigenome luciferase reporter. Similar replication kinetics were observed for H5N1-HaLo in HeLa and 293T cells (Fig. 6C, left). However, we detected lower levels of A/WSN/33 replication in HeLa cells than in 293T cells at 24 hpi (41 relative light units [RLU] in HeLa cells versus 75 RLU in 293T cells [$P \leq 0.001$]) (Fig. 6C, right). Levels of translation of early (PA and NP) and late (M2) IAV proteins were also lower in lysates of HeLa cells infected with A/WSN/33 than those of H5N1-HaLo (Fig. 6D). We also observed lower levels of viral protein translation in A549 cells infected with A/WSN/33 than in those infected with H5N1-HaLo, but to a much lesser extent than in HeLa cells (Fig. 6E). While the observed defects in nuclear import, viral replication, and translation could be the major contributors to abortive H1N1 infection, we cannot conclude that these levels of translation are insufficient to support viral growth and that other late-stage defects ultimately prevent the production of viral particles.

Efficient trafficking of IAV proteins to the host cell membrane is critical for virion assembly and budding. Quantification of HA surface expression in nonpermeabilized HeLa cells infected with the A/WSN/33 virus revealed highly significant reductions at both 16 and 24 hpi relative to expression in infected A549 cells (Fig. 6F). To investigate IAV HA trafficking in more detail, we transfected 293T and HeLa cells with A/WSN/33 (H1N1) or A/Vietnam/1203/04 (H5N1) HA expression constructs and measured HA surface expression in nonpermeabilized cells. No significant differences in the percentage of HA-positive cells were observed between the two cell lines (Fig. 6G), suggesting that trafficking of H1N1 HA is not affected in HeLa cells and that the decreased levels of surface HA observed in A/WSN/33 (H1N1)-infected HeLa cells (Fig. 6F) could be the cumulative result of early reductions in viral import and viral replication. Subsequently, we measured viral budding. No budding virions were observed by transmission electron microscopy in HeLa cells infected with A/WSN/33 (Fig. 6H, center), while progeny virions were detected following infection with H5N1-HaLo (Fig. 6H, bottom). To confirm a deficiency in budding, viral genomic RNA (vRNA) in the supernatants of HeLa and A549 cells infected with A/WSN/33 was quantified, and no NP vRNA was detected in HeLa cell supernatants (Fig. 6I).

H5N1 NP and HA segments enable H1N1 IAV growth in HeLa cells. To identify the H5N1 viral determinant(s) that enables growth in HeLa cells, we generated recombinant A/Puerto Rico/8/1934 (H1N1) (PR8) viruses containing H5N1 genomic segments. All recombinant H1N1-H5N1 viruses were tested for the ability to grow in A549 cells, and the relative replicative fitness of each was compared to that of PR8 in order to rule out recombinant viruses that enhanced infection to levels greater than those with the parental strains (Fig. 7A, B, and C). In the first set of experiments, we introduced either the H5N1 polymerase complex (H5N1 Pol), comprising PB1, PB2, and PA, or H5N1 ribonucleoprotein (H5N1 vRNP), comprising the polymerase complex and NP, into PR8 and tested for viral growth in HeLa cells (Fig. 7D). While no infectious virus was detected after the introduction of the H5N1 polymerase complex, the addition of NP in con-

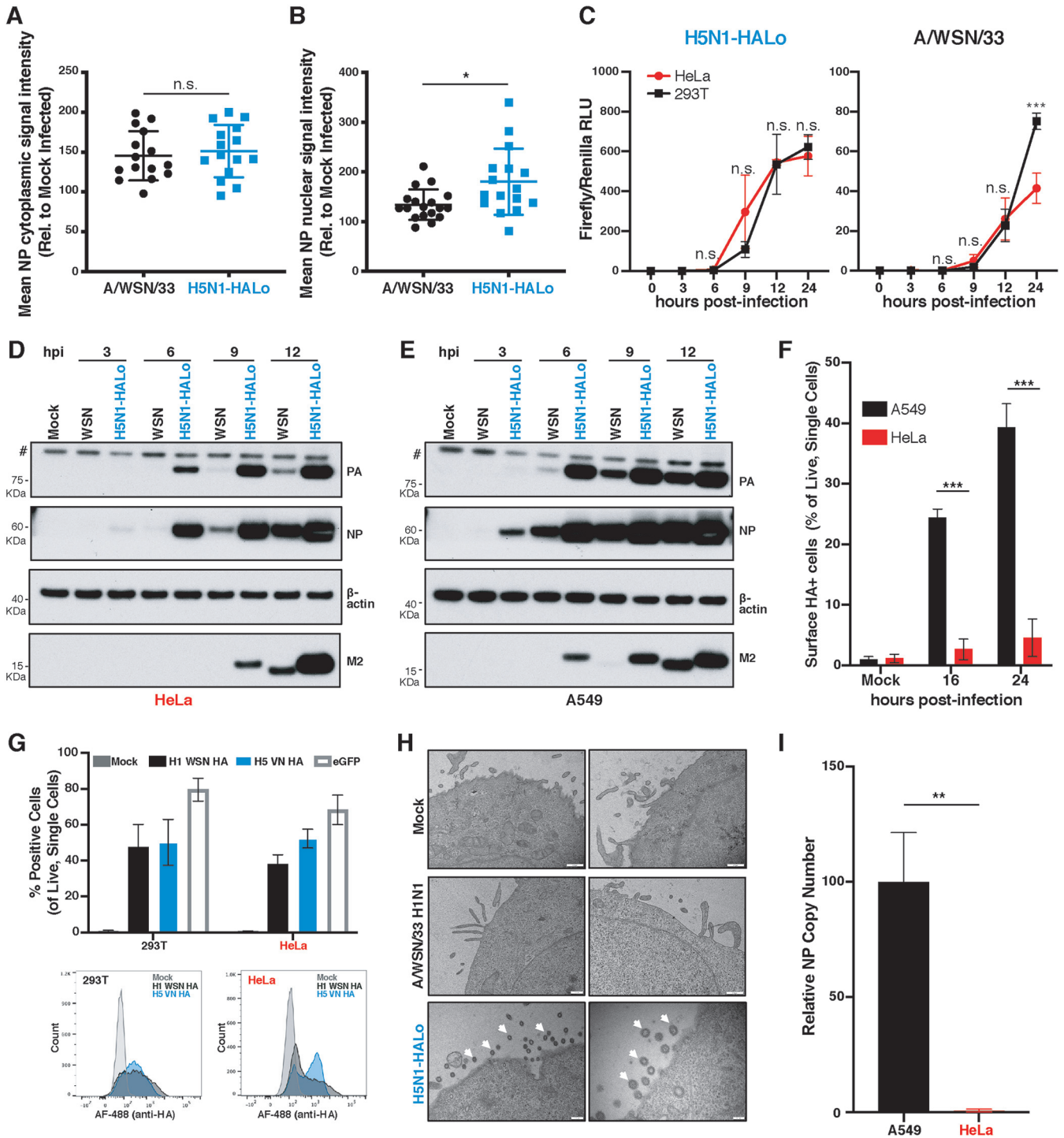


FIG 6 HeLa cells show reduced nuclear import, replication, and translation, as well as deficient budding of H1N1 IAV. (A and B) HeLa cells were synchronously infected with either A/WSN/33 or H5N1-HaLo at an MOI of 10, treated with CHX (100 mg/ml), and then incubated for 3 h at 37°C to allow entry (A) or for 4.5 h at 37°C to allow nuclear import (B). Cells were fixed and stained for IAV NP, and immunofluorescence images were acquired using the IC200 imaging system and were analyzed for cytoplasmic (A) or nuclear (B) NP staining. At least three wells per condition were used, and four fields per well were analyzed for quantification. Circles and squares indicate individual wells assayed, and crossbars indicate mean \pm standard deviation from two independent experiments. Rel., relative; n.s., not significant. (C) An IAV infection-driven minigenome luciferase assay was used to measure polymerase activity in order to monitor infection with either H5N1-HaLo (left) or A/WSN/33 (right) at the indicated time points postinfection in HeLa (solid red lines) or 293T (solid black lines) cells. The firefly luciferase signal was normalized to the expression of *Renilla* luciferase, used as a transfection control. Data are mean \pm standard error of the mean from three independent biological experiments. (D and E) Representative Western blots of protein lysates from HeLa cells (D) or A549 cells (E) infected with A/WSN/33 or H5N1-HaLo at an MOI of 3, collected at 3, 6, 9, and 12 hpi and probed for expression of IAV PA, NP, and M2 proteins and the loading control β -actin. Three independent biological experiments were performed. The number sign (#) indicates a nonspecific band seen under all conditions. (F) HA cell surface staining in nonpermeabilized HeLa (red bars) or A549 (black bars) cells following infection with A/WSN/33 at an MOI of 0.5. The percentage of HA-positive (HA+) cells, (Continued on next page)

junction with H5N1 polymerases led to a 7-fold increase in viral growth at 48 hpi (1×10^2 PFU/ml versus 7.6×10^2 PFU/ml [$P \leq 0.05$]). Next, we introduced H5N1 NS, M, NA, HA, and NP individually into the PR8 virus. Only the recombinant virus bearing H5N1 NP was able to generate detectable levels of infectious virus (Fig. 7E). To determine if H5N1 NP in combination with other viral segments could enhance productive virus infection, we created a series of PR8 viruses that contained H5N1 NP and either M, NS, NA, or HA from an H5N1 virus. Interestingly, the PR8 recombinant virus harboring both the NP and HA segments of an H5N1 virus was able to replicate and produce high virus titers, in contrast to PR8 (5×10^5 PFU/ml versus 1×10^2 PFU/ml at 72 hpi [$P \leq 0.0001$]) (Fig. 7F). Since H5N1 HA and NP were necessary to enable H1N1 growth, we compared HA and NP sequences with those of IAV strains that were unable to grow in HeLa cells and showed that while HA is highly divergent (Fig. 7G), NP is highly conserved (Fig. 7H) across all strains tested. Taken together, these data suggest that viral determinants in H5N1 NP and HA proteins enable replication in otherwise refractory HeLa cells.

DISCUSSION

Influenza A virus tropism is, in part, dictated by the ability of the virus to interact with the cellular landscape. Here, we investigated IAV replication in a diverse subset of human epithelial cell lines with the ultimate aim of identifying determinants of viral growth. We show that epithelial cell lines derived from various tissues are differentially susceptible to multicycle IAV replication and that HeLa cells do not support productive infection by IAV strains of different serotypes and origins, including human H1N1, H3N2, and LPAI viruses. Previous studies have also observed abortive infection with A/Puerto Rico/8/1934 (H1N1), A/WSN/33 (H1N1), A/Texas/1/77 (H3N2), and avian H7N1 (A/fowl plague virus [FPV]/Ulster/73, A/FPV/Rostock/1934) viruses in HeLa cells (31–35). These studies alluded to a block at the level of HA trafficking, viral maturation, and assembly, but the cellular and viral determinants responsible for this phenotype were not further elucidated. Our data show that IAV H1N1 nuclear import, replication, and translation are also affected in HeLa cells. A possible explanation for this discrepancy is that while previous work investigated the ability of IAV to replicate in HeLa cells compared to that in chicken embryo fibroblasts, we compared HeLa cells to other human epithelial cell lines.

Importantly, results from this study reveal that a human isolate of HPAI H5N1 virus replicated successfully in HeLa cells despite abortive infection of a broad range of IAVs of different serotypes and origins and that H5N1 NP and HA are the critical viral determinants that allow replicative fitness in HeLa cells. Finally, our heterokaryon studies suggest that H1N1 viruses, but not H5N1 viruses, require one or more cellular factors that are deficient in HeLa cells. Alternatively, we cannot exclude the possibility that this phenotype is the result of a negative factor(s) in HeLa cells that is diluted or inactivated by another factor present in 293T cells. Comparative transcriptome analyses of IAV-permissive and nonpermissive cells, cross-referenced with published IAV proviral factors (15, 21), may provide a starting point for the investigation of a cellular factor(s) that underlies the observed phenotype in HeLa cells (see Table S1 in the supplemental material).

The introduction of H5N1 NP and HA segments into H1N1 IAV was necessary and

FIG 6 Legend (Continued)

determined by gating of live, single cells and analysis via flow cytometry, is shown. Data are mean \pm standard deviation for three independent experiments. (G) 293T or HeLa cells were transfected with plasmids expressing either A/WSN/33 (H1N1) HA or A/Vietnam/1203/04 (H5N1) HA. Cell surface staining of HA was assessed at 48 h posttransfection by flow cytometry. The percentages of HA⁺ cells are graphed, and histograms of HA⁺ populations following the gating of live, single cells are shown. A plasmid expressing eGFP was transfected alongside the virus-expressing plasmids as a positive control, and mock-transfected cells served as negative controls. Data are mean \pm standard deviation from three independent experiments. (H) HeLa cells were either mock infected or infected at an MOI of 1 with A/WSN/33 or H5N1-HaLo. At 10 hpi, cells were fixed, negatively stained with uranyl acetate, and visualized by transmission electron microscopy. Arrows indicate newly released influenza virions. (I) A549 or HeLa cells were infected with A/WSN/33 at an MOI of 0.01, and supernatant samples were collected at 72 hpi for extraction of total viral RNA. Genomic copies of NP were quantified by qRT-PCR in three independent biological experiments. Asterisks indicate significant differences by multiple Student *t* tests (*, $P \leq 0.05$; **, $P \leq 0.001$; ***, $P \leq 0.0001$).

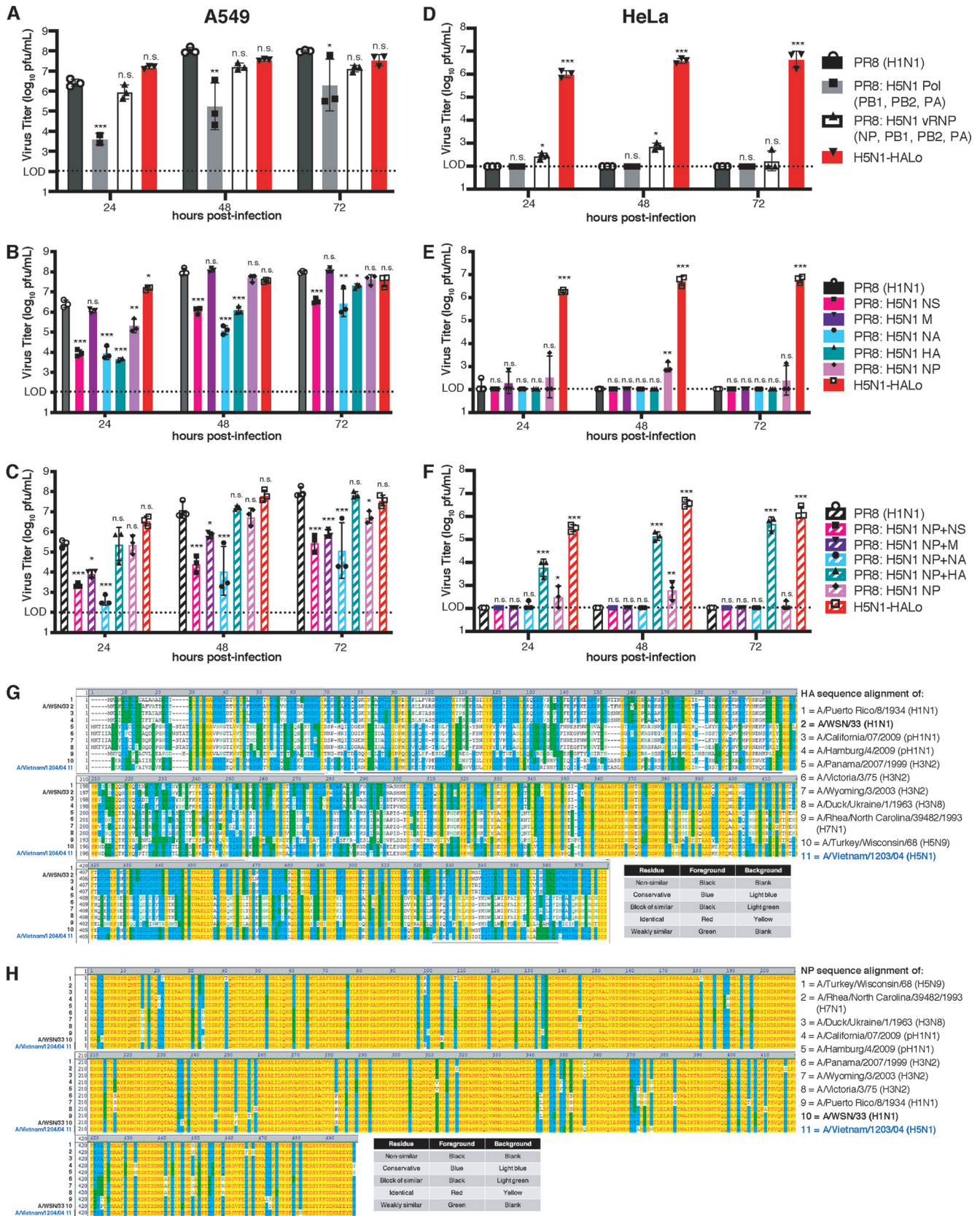


FIG 7 H5N1 NP and HA segments enable H1N1 IAV growth in HeLa cells. Recombinant viruses were created using the A/Puerto Rico/8/1934 (H1N1) [PR8 (H1N1)] backbone and introducing the indicated segment(s) of the H5N1 IAV. (A through F) A549 (left) or HeLa (right) cells were infected with recombinant viruses at an MOI of 0.01 to test the effect of the H5N1 polymerase complex (PB1, PB2, and PA) or the viral ribonucleoprotein (vRNP) complex (PB1, PB2, PA, (Continued on next page)

sufficient to enable growth in HeLa cells. During influenza virus infection, NP is imported to the nucleus, where it drives viral replication and transcription. In contrast, HA is important for the entry and budding of influenza viruses. We therefore hypothesize that determinants in the H5N1 NP might be responsible for increased nuclear import and replication in HeLa cells, while determinants in H5N1 HA might be responsible for efficient budding. The initiation of IAV virion budding relies on the interaction of membrane-bound HA with host cell membrane lipid rafts and viral membrane proteins (NA, M1, and M2) (reviewed in reference 41). Therefore, the absence of virion budding from HeLa cells following H1N1 infection could be due to defective recruitment of one or more viral factors to the plasma membrane and/or the inability of HA to initiate viral budding. However, at this moment, we cannot exclude the possibility that defects in nuclear import, viral replication, and translation are the major contributors to abortive H1N1 infection or that other, alternative mechanisms are responsible for the rescue of the growth of the PR8 (H1N1) virus in HeLa cells by H5N1 HA and NP genes.

NP, HA, and the viral polymerases have been described as determinants of the host range specificity and pathogenicity of HPAI viruses (23, 26). NP nuclear import depends on efficient interaction with cellular importins. Adaptive mutations in avian IAV NP proteins allow a switch from utilization of importin- α 3 to importin- α 7 for efficient nuclear import in mammalian cells and host range expansion (42, 43). The acquisition of a polybasic cleavage site in HA extends the tissue tropism of the virus and facilitates systemic infection (27, 28). Acquired mutations in the viral polymerases of avian IAVs enable efficient replication in mammalian cells (reviewed in references 23 and 44). A well-studied mutation is the E627K substitution in the PB2 polymerase protein, which has been reported in H5N1 human isolates (45–48; for a review, see reference 45). Of note, the A/Vietnam/1203/2004 (H5N1) HA_{Lo} virus used in our studies has this E627K amino acid substitution in its PB2 segment (49). This mutation confers high levels of viral polymerase activity in human cells, a characteristic that we also observed in our minigenome-based assay following H5N1-HA_{Lo} infection (Fig. 6C). In addition, this mutation changes the ability of the polymerase to functionally interact with mammalian cellular factors such as ANP32A, ANP32B, and DDX17 (20, 24; reviewed in reference 44). Therefore, it is possible that successful H5N1 viral growth in HeLa cells could be mediated by determinants in HA and NP that facilitate interaction with a broader range of host factors in HeLa cells, enabling H5N1 viruses to replicate despite the absence of a host factor(s) essential for the growth of other IAV strains.

Alternatively, H5N1 viruses may induce the expression of a distinct profile of host genes, altering the cellular landscape. Comparison of the global transcriptome upon H1N1, H3N2, or H5N1 virus infection has revealed significant differences in host gene expression and host proteomic responses between these strains (50, 51). Thus, H5N1 virus infection may reshape the cellular milieu to promote a host factor environment that enables productive replication in HeLa cells. Cross-strain transcriptome analyses of HeLa cells that are either uninfected or infected with the WSN or H5N1-HA_{Lo} virus and cross-referenced with previously identified pro-IAV factors (15, 21) might additionally facilitate the discovery of these cellular factors (see Table S2 in the supplemental material).

Taking our findings together, our study provides a survey of IAV growth in different human epithelial cell lines. Abortive infection with H1N1, H3N2, and LPAI viruses, but not H5N1, was attributable to a cellular defect in HeLa cells. Importantly, viral features

FIG 7 Legend (Continued)

and NP) (A and D), the effects of individual H5N1 gene segments (B and E), or the combinatorial effect of the H5N1 NP with other H5N1 gene segments (C and F) on virus growth. At the indicated times, infectious virus release was determined by plaque assay. Bars represent mean \pm standard deviation from at least three independent biological experiments, while each symbol represents the mean value from an independent experiment. The limit of detection (LOD) for the plaque assay is indicated by a dotted black line at 1×10^2 PFU/ml. Asterisks indicate significant differences (*, $P \leq 0.05$; **, $P \leq 0.001$; ***, $P \leq 0.0001$) by two-way analysis of variance, with Dunnett's multiple-comparison test for comparisons to PR8. (G and H) Full nucleotide sequence alignments of the HA (G) and NP (H) gene segments from the indicated IAV strains.

in H5N1 NP and HA enabled H1N1 viral growth in HeLa cells, likely relieving the dependency on one or more cellular factors or functions. Further investigation of these host and viral determinants is likely to reveal critical host-pathogen interactions that govern IAV replication and pathogenesis.

MATERIALS AND METHODS

Cells. A549 (ATCC CCL-185), MDCK (ATCC CCL-34), 293T (ATCC CRL-3216), HeLa (ATCC CCL-2), and Huh-7 cells were cultured in Dulbecco's modified Eagle medium (DMEM). SK-N-SH, U87-CD4-CXCR4, and HOS-CD4 cells were cultured in minimal essential medium (MEM). HCT15 cells were cultured in RPMI medium, and U2OS cells were cultured in McCoy's medium. All culture media were supplemented with 10% fetal bovine serum (FBS), 1% penicillin-streptomycin-glutamine, 1% HEPES, and 1% sodium pyruvate. Cells were grown at 37°C under 5% CO₂. All cell lines were routinely tested for mycoplasma contamination.

Generation of HeLa-mCherry and 293T-zsGreen cells. HeLa and 293T cells were transduced with pTripz-scr-Dox/pCDNA-Puro-mCherry or plx304-zsGreen lentiviral vectors, respectively. At 48 h posttransduction, HeLa cells were subjected to antibiotic selection in culture media with 0.5 µg/ml puromycin (Invitrogen), whereas 293T cells were selected with 10 µg/ml blasticidin (Invitrogen), to establish a population of transduced fluorescent cells. Before stable cell populations were frozen, each cell line was FACS sorted for purity on a FACSAria II flow cytometer (BD Biosciences) and was gated for live, single cells and for mCherry or zsGreen expression.

Generation of HeLa-293T cell heterokaryons. HeLa-mCherry and 293T-zsGreen cells were used to generate heterokaryons as described in reference 40. Briefly, HeLa-mCherry and 293T-zsGreen were plated onto 10-cm poly-D-lysine (ICN102694; Fisher Scientific)-coated tissue culture dishes in DMEM with 10% FBS, 1% HEPES, and 1% sodium pyruvate and were transfected with VSV-G by using FuGENE 6 according to the manufacturer's guidelines (Promega). At 48 h posttransfection, cells were harvested by trypsinization and were counted. In a 15-cm poly-D-lysine-coated tissue culture dish, transfected HeLa-mCherry cells and 293T-zsGreen cells were plated together at a 2:1 ratio and were incubated for 4 h to allow adherence. The cell culture medium was then removed. Cells were washed with 1× Dulbecco's phosphate-buffered saline (DPBS), exposed to pH 6.0 for 3 min in fusion buffer [1 M 2-(N-morpholino)ethanesulfonic acid (MES) (product no. M1317; Sigma) in 1× DPBS (12.5 ml MES per liter 1× DPBS)], and then incubated in complete culture medium comprising DMEM, 10% FBS, 1% HEPES, 1% sodium pyruvate, and 1% penicillin-streptomycin-L-glutamine. At 36 to 48 h postfusion, cells were harvested by trypsinization, washed, resuspended in FACS sorting buffer (1× PBS [Ca²⁺ and Mg²⁺ free], 20 mM HEPES [pH 7.2], 1% bovine serum albumin [BSA], 2 mM EDTA), and sorted on a FACSAria II flow cytometer (BD Biosciences) using a 130-µm nozzle at 4°C. Cells were gated for live, single cells, and zsGreen^{hi} mCherry^{hi} and zsGreen^{low} mCherry^{hi} double-positive cells were collected in complete culture medium for infection experiments (as depicted in Fig. 5B). Gating criteria were set up to stringently exclude zsGreen single-positive cells.

Viruses. The influenza virus strains A/WSN/33 (H1N1), A/Puerto Rico/8/1934 (H1N1), A/California/07/2009 (pH1N1), A/Hamburg/4/2009 (pH1N1), A/Victoria/3/75 (H3N2), A/Wyoming/3/2003 (H3N2), A/Panama/2007/1999 (H3N2), A/Duck/Ukraine/1/1963 (H3N8), A/Turkey/Wisconsin/68 (H5N9), A/Rhea/North Carolina/39482/1993 (H7N1), and A/Vietnam/1203/2004 HALo (H5N1) were propagated in embryonated eggs and titrated in MDCK cells. The C13 GFP_P2A_NP recombinant lymphocytic choriomeningitis virus (rLCMV) was kindly provided by J. C. de la Torre (The Scripps Research Institute, La Jolla, CA). The MHV-68 luciferase reporter virus was provided by R. Sun and T.-T. Wu (University of California, Los Angeles). Dengue virus strain 16681 was kindly provided by M. Diamond (Washington University, St. Louis, MO).

Generation of recombinant H1N1 and H5N1 influenza A viruses. Recombinant influenza viruses were developed by reverse genetics as described previously (52, 53) and were propagated in embryonated eggs. The genotypes of these viruses were verified using Sanger sequencing (Macrogen).

Virus infection. Cells were infected with viruses, at the multiplicities of infection stated in the figure legends, in PBS supplemented with BSA, Ca²⁺, and Mg²⁺. After 1 h, cells were washed, and a culture medium containing 1 µg/ml tosylsulfonyl phenylalanyl chloromethyl ketone (TPCK)-treated trypsin was added. Cells were then incubated at 37°C and supernatant samples collected at the times indicated in the figure legends. Viral titers in supernatants were determined by plaque assay using MDCK cells.

Influenza A virus entry and nuclear import assays. HeLa cells were infected with influenza virus A/WSN/33 or H5N1-HaLo at an MOI of 10 for 1 h on ice. Cells were then washed and were incubated in culture medium at 37°C under 5% CO₂ in the presence of cycloheximide (100 mg/ml). For entry assays, cells were fixed after 3 h, and for nuclear import quantification, cells were fixed after 4.5 h. Cells stained for IAV NP (with Alexa Fluor 488), DNA (with 4',6-diamidino-2-phenylindole [DAPI]), and cytoplasm (HCS CellMask) were imaged using the IC200 imaging system (Vala Sciences, San Diego, CA) at a magnification of ×20, with four fields imaged per well. Multiparametric image analysis was performed using Columbus software, version 2.5 (PerkinElmer). The DAPI signal was used to detect cellular nuclei and the HCS CellMask Deep Red channel to delineate the cellular cytoplasm. Signal intensities for Alexa Fluor 488 (used to detect IAV NP) in the cytoplasm and in the nucleus were then calculated.

Influenza virus polymerase activity assays. HeLa and 293T cells were transfected with an influenza virus-like minigenome encoding negative-sense firefly luciferase and the internal control *Renilla* luciferase (kindly provided by Wendy Barclay, Imperial College London, London, UK). At 24 h posttransfection, cells were infected with influenza virus A/WSN/33 (H1N1) or H5N1-HaLo at an MOI of 3 for the times

shown in Fig. 6. Firefly luciferase and *Renilla* luciferase levels were measured using a Dual-Glo luciferase assay (Promega).

Flow cytometry analysis of HA expression. HeLa and A549 cells were either mock treated or infected with influenza virus A/WSN/33 at an MOI of 0.5 and were incubated for either 16 or 24 h. Cells were trypsinized, washed in 1× DPBS (Gibco) with 3% FBS, and blocked for 2 h in PBS with a 1:200 dilution of normal rabbit serum (ab7487; Abcam). Membrane-bound (surface) HA was stained using an anti-IAV H1N1 HA antibody (clone C102; catalog no. GTX28262; GeneTex) overnight at 4°C in 1× DPBS (Gibco) with 3% FBS. Cells were then stained with an Alexa-Fluor 568-conjugated goat anti-mouse secondary antibody (Thermo Fisher Scientific) for 2 h at room temperature, washed, and fixed in 4% paraformaldehyde in PBS for 20 min at room temperature. For HA overexpression experiments, 293T and HeLa cells were transfected with either pDZ-WSN H1 HA, pCAGGS-Vietnam/1203 H5 HA, or enhanced green fluorescent protein (eGFP) by using the FuGENE 6 reagent (Promega) according to the manufacturer's protocol. At 48 h posttransfection, cells were trypsinized, washed in 1× DPBS (Gibco) with 3% FBS, and stained for membrane-bound (surface) HA using an IAV universal human monoclonal antibody (CR9114) at 1:1,000 for 1 h at room temperature. Cells were then stained with an Alexa Fluor 488-conjugated goat anti-human secondary antibody (Thermo Fisher Scientific) for 30 min at room temperature, washed, and fixed in 4% paraformaldehyde in PBS for 20 min at room temperature. All samples were run on an Attune NxT flow cytometer (Thermo Fisher Scientific). The resulting data were analyzed using FlowJo software (Tree Star).

Transmission electron microscopy. HeLa cells were grown in DMEM in 35-mm culture dishes. Following infection at an MOI of 1 with influenza virus A/WSN/33 or H5N1-HaLo and incubation for 12 h, the medium was removed, and the cells were fixed in a solution of 2.5% glutaraldehyde in 0.1 M sodium cacodylate buffer, pH 7.3 (2 ml per dish), at 4°C overnight. After fixation, the cells were washed three times in 0.1 M sodium cacodylate buffer, pH 7.3, at room temperature for 10 min each time. The cells were then postfixed in 1.0% OsO₄ in 0.1 M sodium cacodylate buffer at room temperature for 1 h, followed by three washes in 0.1 M sodium cacodylate buffer for 10 min each. Subsequently, cells were treated with 0.5% tannic acid in 0.05 M cacodylate buffer for 30 min. Cells were then rinsed in 1% Na₂SO₄ in 0.1 M cacodylate buffer for 10 min, followed by a wash in 0.1 M cacodylate buffer for 10 min. Cells were dehydrated through a graded ethanol series (30%, 50%, 70%, 90%, and 100%) for 10 min at each step. Following dehydration, the samples were transitioned through HPMA (2-hydroxypropyl methacrylate) twice for 15 min at each step. The samples were infiltrated with LX-112 resin (approximately 2 ml per dish) overnight at room temperature. The next morning, the resin was replaced with fresh LX-112, and the dishes were transferred to a 60°C oven for 48 h. Sections (thickness, 70 nm) were cut (using a Reichert Ultracut E ultramicrotome), collected on copper mesh grids, and stained with uranyl acetate followed by lead citrate. Images were taken using an FEI CM100 transmission electron microscope equipped with a Soft Imaging System MegaView III charge-coupled device (CCD) camera.

Determination of viral RNA copy numbers. Viral RNA was extracted using the QIAamp viral RNA minikit (Qiagen Sciences) and was reverse transcribed with SuperScript III reverse transcriptase (Thermo Fisher). Quantitative real-time PCR was performed using the Power Sybr green master mix (Applied Biosystems, Inc. [ABI]) on the ViiA 7 real-time PCR system (ABI). For viral copy numbers, a standard curve ranging from 1 × 10⁰ to 1 × 10⁸ was used for quantification. The primers used were WSN-NP-Fwd (GACGATGCAACGGCTGGTCTG) and WSN-NP-Rev (ACCATTGTCCAATCCTTT) (54).

SDS-PAGE and immunoblotting. Cells were washed once with DPBS, and lysates were collected in 2× NuPage LDS (lithium dodecyl sulfate) sample buffer (catalog no. NP0007; Thermo Fisher) and were boiled for 10 min at 95°C. Protein samples were separated using SDS-polyacrylamide gel electrophoresis and were further immunoblotted with the following primary antibodies: a rabbit polyclonal antibody against PA (catalog no. GTX118991; GeneTex), a rabbit polyclonal antibody against NP (described in reference 55), a mouse monoclonal antibody against M2 (catalog no. sc-32238; Santa Cruz), and a rabbit monoclonal antibody against β-actin (product no. 4970; Cell Signaling).

RNA-seq. RNA-seq of mock-infected A549 or HeLa cells and of HeLa cells infected with influenza virus A/WSN/33 (H1N1) or H5N1-HaLo were prepared as follows. Cells were mock infected or infected with the A/WSN/33 or H5N1-HaLo virus at an MOI of 3. After 1 h, cells were first washed and then incubated with medium at 37°C. After 9 h, cell extracts were collected with TRIzol, and total RNA was extracted using an RNeasy minikit (Qiagen). Strand-specific poly(A)-selected sequencing libraries were produced according to standard Illumina protocols, and sequencing was carried out on an Illumina HiSeq 4000 system. Sequencing reads were aligned to the human GRCh38 and HPV18 genomes with STAR (56). The genome sequence and gene annotation were based on RefSeq assembly accession no. GCF_000865665.1. Normalized gene expression (fragments per kilobase of transcript per million mapped reads [FPKM]) was calculated based on total uniquely mapped reads to human and viral genomes for each sample.

DNA and siRNA transfections. DNA transfections of 293T cells were performed using the FuGENE 6 (Promega) reagent according to the manufacturer's protocol. For siRNA transfections, HeLa or A549 cells were reverse transfected in suspension with 30 nM siRNA (Qiagen) diluted in Opti-MEM (Life Technologies) using the RNAiMAX reagent according to the manufacturer's protocol (Invitrogen). At 48 h posttransfection, either cells were infected, and productive virus growth was measured by plaque assay, or cell viability was determined using the CellTiter-Glo assay (Promega).

RNA extraction and quantitative reverse transcription-PCR (qRT-PCR). At 48 h post-siRNA transfection, total RNA was extracted from HeLa cells using an RNeasy minikit (Qiagen). A high-capacity RNA-to-cDNA kit (ABI) and the Power Sybr green master mix (ABI) were used to quantify HPV18 E1, HPV18 E6, HPV18 E7, HPV18 L1, and TATA binding protein (TBP) mRNAs on the ViiA 7 real-time PCR system (ABI). Each HPV18 mRNA was normalized to TBP mRNA, which was used as the reference gene.

The following primers were used: for HPV18 E1, 5'-ANANGCTGTGCAGKNNCTAAAACGAAG-3' and 5'-AGTTCCACTTCAGTATTGCCATA-3' (57); for HPV18 E6, 5'-CGCGCTTTGAGGATCCAA-3' and 5'-TATGGCATG CAGCATGGG-3' (58); for HPV18 E7, 5'-GCTAGCATATGCATGGACCTAAGGCAAC-3' and 5'-TCTAGATTACT GCTGGGATGCACACC-3' (58); for HPV18 L1, 5'-GCATAATCAATTATTTGTTACTGTGGTAGATACCACT-3' and 5'-GCTATACTGCTAAATTTGGTAGCATCATATTCG-3' (57); and for TBP, 5'-CCACTCACAGACTCTACAAC-3' and 5'-CTGCGGTACAATCCCAGAACT-3' (59).

Data availability. The A549 and HeLa cell RNA-seq data used in this study have been deposited in the Gene Expression Omnibus (GEO) database repository under accession number GSE140759.

SUPPLEMENTAL MATERIAL

Supplemental material is available online only.

SUPPLEMENTAL FILE 1, XLSX file, 4.2 MB.

SUPPLEMENTAL FILE 2, XLSX file, 7.8 MB.

ACKNOWLEDGMENTS

We thank Juan Carlos de la Torre for providing the LCMV reporter virus, Ren Sun and Ting-Ting Wu for providing the MHV-68 luciferase reporter virus, Michael S. Diamond for providing Huh-7 cells and strain 16681 of dengue virus, and Wendy Barclay for providing the influenza virus-like minigenome reporter. We also thank Amy Cortez and Yoav Altman in the Sanford Burnham Prebys Flow Cytometry Core for technical assistance with FACS sorting of the heterokaryons and Debbie Chen and Susanne Heynen-Genel for assistance with the IC200 imaging system.

This work was supported by NIH/NIAID research grant U19 AI12027 to A.G.-S., C.B., and S.K.C. This work was also partly supported by NIAID grant U19AI117873 and by CRIP (Center for Research on Influenza Pathogenesis), a NIAID-funded Center of Excellence for Influenza Research and Surveillance (CEIRS; contract HHSN272201400008C) (to A.G.-S.). A.P.G. was supported by the Sanford Burnham Prebys Frontiers in Immunology training grant (T32 AI 125209-1). This work was also supported by a generous grant from the James B. Pendleton Charitable Trust.

REFERENCES

- Palese P, Shaw ML. 2007. Orthomyxoviridae: the viruses and their replication, p 1647–1690. *In* Knipe DM, Howley PM, Griffin DE, Lamb RA, Martin MA, Roizman B, Straus SE (ed), *Fields virology*, 5th ed. Lippincott Williams & Wilkins, Philadelphia, PA.
- Molinari NA, Ortega-Sanchez IR, Messonnier ML, Thompson WW, Wortley PM, Weintraub E, Bridges CB. 2007. The annual impact of seasonal influenza in the US: measuring disease burden and costs. *Vaccine* 25: 5086–5096. <https://doi.org/10.1016/j.vaccine.2007.03.046>.
- CDC. 2019. Disease burden of influenza. <https://www.cdc.gov/flu/about/burden/index.html>.
- Klenk HD. 2014. Influenza viruses en route from birds to man. *Cell Host Microbe* 15:653–654. <https://doi.org/10.1016/j.chom.2014.05.019>.
- Lycett SJ, Duchatel F, Digard P. 2019. A brief history of bird flu. *Philos Trans R Soc Lond B Biol Sci* 374:20180257. <https://doi.org/10.1098/rstb.2018.0257>.
- WHO. 2019. Cumulative number of confirmed human cases for avian influenza A(H5N1) reported to WHO, 2003–2019. https://www.who.int/influenza/human_animal_interface/2019_06_24_tableH5N1.pdf?ua=1.
- Herfst S, Schrauwen EJ, Linster M, Chutinimitkul S, de Wit E, Munster VJ, Sorrell EM, Bestebroer TM, Burke DF, Smith DJ, Rimmelzwaan GF, Osterhaus AD, Fouchier RA. 2012. Airborne transmission of influenza A/H5N1 virus between ferrets. *Science* 336:1534–1541. <https://doi.org/10.1126/science.1213362>.
- Imai M, Watanabe T, Hatta M, Das SC, Ozawa M, Shinya K, Zhong G, Hanson A, Katsura H, Watanabe S, Li C, Kawakami E, Yamada S, Kiso M, Suzuki Y, Maher EA, Neumann G, Kawaoka Y. 2012. Experimental adaptation of an influenza H5 HA confers respiratory droplet transmission to a reassortant H5 HA/H1N1 virus in ferrets. *Nature* 486:420–428. <https://doi.org/10.1038/nature10831>.
- Sorrell EM, Schrauwen EJ, Linster M, De Graaf M, Herfst S, Fouchier RA. 2011. Predicting 'airborne' influenza viruses: (trans-) mission impossible? *Curr Opin Virol* 1:635–642. <https://doi.org/10.1016/j.coviro.2011.07.003>.
- Krammer F, Smith GJD, Fouchier RAM, Peiris M, Kedzierska K, Doherty PC, Palese P, Shaw ML, Treanor J, Webster RG, Garcia-Sastre A. 2018. Influenza. *Nat Rev Dis Primers* 4:3. <https://doi.org/10.1038/s41572-018-0002-y>.
- Hao L, Sakurai A, Watanabe T, Sorensen E, Nidom CA, Newton MA, Ahlquist P, Kawaoka Y. 2008. *Drosophila* RNAi screen identifies host genes important for influenza virus replication. *Nature* 454:890–893. <https://doi.org/10.1038/nature07151>.
- Karlas A, Machuy N, Shin Y, Pleissner KP, Artarini A, Heuer D, Becker D, Khalil H, Ogilvie LA, Hess S, Maurer AP, Muller E, Wolff T, Rudel T, Meyer TF. 2010. Genome-wide RNAi screen identifies human host factors crucial for influenza virus replication. *Nature* 463:818–822. <https://doi.org/10.1038/nature08760>.
- Konig R, Stertz S, Zhou Y, Inoue A, Hoffmann HH, Bhattacharyya S, Alamares JG, Tscherne DM, Ortigoza MB, Liang Y, Gao Q, Andrews SE, Bandyopadhyay S, De Jesus P, Tu BP, Pache L, Shih C, Orth A, Bonamy G, Miraglia L, Ideker T, Garcia-Sastre A, Young JA, Palese P, Shaw ML, Chanda SK. 2010. Human host factors required for influenza virus replication. *Nature* 463:813–817. <https://doi.org/10.1038/nature08699>.
- Shapira SD, Gat-Viks I, Shum BO, Dricot A, de Grace MM, Wu L, Gupta PB, Hao T, Silver SJ, Root DE, Hill DE, Regev A, Hacohen N. 2009. A physical and regulatory map of host-influenza interactions reveals pathways in H1N1 infection. *Cell* 139:1255–1267. <https://doi.org/10.1016/j.cell.2009.12.018>.
- Han J, Perez JT, Chen C, Li Y, Benitez A, Kandasamy M, Lee Y, Andrade J, tenOever B, Manicassamy B. 2018. Genome-wide CRISPR/Cas9 screen identifies host factors essential for influenza virus replication. *Cell Rep* 23:596–607. <https://doi.org/10.1016/j.celrep.2018.03.045>.
- Mehle A, Doudna JA. 2008. An inhibitory activity in human cells restricts the function of an avian-like influenza virus polymerase. *Cell Host Microbe* 4:111–122. <https://doi.org/10.1016/j.chom.2008.06.007>.
- Kuo SM, Chen CJ, Chang SC, Liu TJ, Chen YH, Huang SY, Shih SR. 2017. Inhibition of avian influenza A virus replication in human cells by host restriction factor TUFM is correlated with autophagy. *MBio* 8:e00481-17. <https://doi.org/10.1128/mBio.00481-17>.
- Laguette N, Sobhian B, Casartelli N, Ringear M, Chable-Bessia C, Segal

- E, Yatim A, Emiliani S, Schwart O, Benkirane M. 2011. SAMHD1 is the dendritic- and myeloid-cell-specific HIV-1 restriction factor counteracted by Vpx. *Nature* 474:654–657. <https://doi.org/10.1038/nature10117>.
19. Brass AL, Huang IC, Benita Y, John SP, Krishnan MN, Feeley EM, Ryan BJ, Weyer JL, van der Weyden L, Fikrig E, Adams DJ, Xavier RJ, Farzan M, Elledge SJ. 2009. The IFITM proteins mediate cellular resistance to influenza A H1N1 virus, West Nile virus, and dengue virus. *Cell* 139:1243–1254. <https://doi.org/10.1016/j.cell.2009.12.017>.
 20. Long JS, Giotis ES, Moncorge O, Frise R, Mistry B, James J, Morisson M, Iqbal M, Vignal A, Skinner MA, Barclay WS. 2016. Species difference in ANP32A underlies influenza A virus polymerase host restriction. *Nature* 529:101–104. <https://doi.org/10.1038/nature16474>.
 21. Tripathi S, Pohl MO, Zhou Y, Rodriguez-Frandsen A, Wang G, Stein DA, Moulton HM, DeJesus P, Che J, Mulder LCF, Yangüez E, Andenmatten D, Pache L, Manicassamy B, Albrecht RA, Gonzalez MG, Nguyen Q, Brass A, Elledge S, White M, Shapira S, Hacohen N, Karlas A, Meyer TF, Shales M, Gatorano A, Johnson JR, Jang G, Johnson T, Verschueren E, Sanders D, Krogan N, Shaw M, König R, Stertz S, García-Sastre A, Chanda SK. 2015. Meta- and orthogonal integration of influenza “OMICs” data defines a role for UBR4 in virus budding. *Cell Host Microbe* 18:723–735. <https://doi.org/10.1016/j.chom.2015.11.002>.
 22. Moncorge O, Mura M, Barclay WS. 2010. Evidence for avian and human host cell factors that affect the activity of influenza virus polymerase. *J Virol* 84:9978–9986. <https://doi.org/10.1128/JVI.01134-10>.
 23. Cauldwell AV, Long JS, Moncorge O, Barclay WS. 2014. Viral determinants of influenza A virus host range. *J Gen Virol* 95:1193–1210. <https://doi.org/10.1099/vir.0.062836-0>.
 24. Bortz E, Westera L, Maamary J, Steel J, Albrecht RA, Manicassamy B, Chase G, Martínez-Sobrido L, Schwemmler M, García-Sastre A. 2011. Host- and strain-specific regulation of influenza virus polymerase activity by interacting cellular proteins. *MBio* 2:e00151-11. <https://doi.org/10.1128/mBio.00151-11>.
 25. Hudjetz B, Gabriel G. 2012. Human-like PB2 627K influenza virus polymerase activity is regulated by importin- α 1 and - α 7. *PLoS Pathog* 8:e1002488. <https://doi.org/10.1371/journal.ppat.1002488>.
 26. Rodriguez-Frandsen A, Alfonso R, Nieto A. 2015. Influenza virus polymerase: functions on host range, inhibition of cellular response to infection and pathogenicity. *Virus Res* 209:23–38. <https://doi.org/10.1016/j.virusres.2015.03.017>.
 27. Garten W, Klenk HD. 1999. Understanding influenza virus pathogenicity. *Trends Microbiol* 7:99–100. [https://doi.org/10.1016/s0966-842x\(99\)01460-2](https://doi.org/10.1016/s0966-842x(99)01460-2).
 28. Stieneke-Grober A, Vey M, Angliker H, Shaw E, Thomas G, Roberts C, Klenk HD, Garten W. 1992. Influenza virus hemagglutinin with multibasic cleavage site is activated by furin, a subtilisin-like endoprotease. *EMBO J* 11:2407–2414. <https://doi.org/10.1002/j.1460-2075.1992.tb05305.x>.
 29. de Wit E, Kawaoka Y, de Jong MD, Fouchier RA. 2008. Pathogenicity of highly pathogenic avian influenza virus in mammals. *Vaccine* 26(Suppl 4):D54–D58. <https://doi.org/10.1016/j.vaccine.2008.07.072>.
 30. Schrauwen EJ, de Graaf M, Herfst S, Rimmelzwaan GF, Osterhaus AD, Fouchier RA. 2014. Determinants of virulence of influenza A virus. *Eur J Clin Microbiol Infect Dis* 33:479–490. <https://doi.org/10.1007/s10096-013-1984-8>.
 31. Lerner RA, Hodge LD. 1969. Nonpermissive infections of mammalian cells: synthesis of influenza virus genome in HeLa cells. *Proc Natl Acad Sci U S A* 64:544–551. <https://doi.org/10.1073/pnas.64.2.544>.
 32. Caligiuri LA, Holmes KV. 1979. Host-dependent restriction of influenza virus maturation. *Virology* 92:15–30. [https://doi.org/10.1016/0042-6822\(79\)90211-3](https://doi.org/10.1016/0042-6822(79)90211-3).
 33. Portincasa P, Conti G, Chezzi C. 1990. Abortive replication of influenza A viruses in HeLa 229 cells. *Virus Res* 18:29–40. [https://doi.org/10.1016/0168-1702\(90\)90087-r](https://doi.org/10.1016/0168-1702(90)90087-r).
 34. Portincasa P, Conti G, Chezzi C. 1991. Defective insertion of haemagglutinin as a cause of abortivity of influenza A viruses in HeLa 229 cells. *Microbiologica* 14:351–355.
 35. Choppin PW, Pons MW. 1970. The RNAs of infective and incomplete influenza virions grown in MDBK and HeLa cells. *Virology* 42:603–610. [https://doi.org/10.1016/0042-6822\(70\)90306-5](https://doi.org/10.1016/0042-6822(70)90306-5).
 36. Park MS, Steel J, Garcia-Sastre A, Swayne D, Palese P. 2006. Engineered viral vaccine constructs with dual specificity: avian influenza and Newcastle disease. *Proc Natl Acad Sci U S A* 103:8203–8208. <https://doi.org/10.1073/pnas.0602566103>.
 37. Macville M, Schrock E, Padilla-Nash H, Keck C, Ghadimi BM, Zimonjic D, Popescu N, Ried T. 1999. Comprehensive and definitive molecular cytogenetic characterization of HeLa cells by spectral karyotyping. *Cancer Res* 59:141–150.
 38. Schwarz E, Freese UK, Gissmann L, Mayer W, Roggenbuck B, Stremlau A, zur Hausen H. 1985. Structure and transcription of human papillomavirus sequences in cervical carcinoma cells. *Nature* 314:111–114. <https://doi.org/10.1038/314111a0>.
 39. Meissner JD. 1999. Nucleotide sequences and further characterization of human papillomavirus DNA present in the CaSki, SiHa and HeLa cervical carcinoma cell lines. *J Gen Virol* 80:1725–1733. <https://doi.org/10.1099/0022-1317-80-7-1725>.
 40. Gottesman A, Milazzo J, Lazebnik Y. 2010. V-fusion: a convenient, non-toxic method for cell fusion. *Biotechniques* 49:747–750. <https://doi.org/10.2144/000113515>.
 41. Dou D, Revol R, Ostbye H, Wang H, Daniels R. 2018. Influenza A virus cell entry, replication, virion assembly and movement. *Front Immunol* 9:1581. <https://doi.org/10.3389/fimmu.2018.01581>.
 42. Gabriel G, Herwig A, Klenk HD. 2008. Interaction of polymerase subunit PB2 and NP with importin α 1 is a determinant of host range of influenza A virus. *PLoS Pathog* 4:e11. <https://doi.org/10.1371/journal.ppat.0040011>.
 43. Gabriel G, Klingel K, Otte A, Thiele S, Hudjetz B, Arman-Kalcek G, Sauter M, Schmidt T, Rother F, Baumgarte S, Keiner B, Hartmann E, Bader M, Brownlee GG, Fodor E, Klenk HD. 2011. Differential use of importin- α isoforms governs cell tropism and host adaptation of influenza virus. *Nat Commun* 2:156. <https://doi.org/10.1038/ncomms1158>.
 44. Long JS, Mistry B, Haslam SM, Barclay WS. 2019. Host and viral determinants of influenza A virus species specificity. *Nat Rev Microbiol* 17:67–81. <https://doi.org/10.1038/s41579-018-0115-z>.
 45. Gabriel G, Czudai-Matwich V, Klenk HD. 2013. Adaptive mutations in the H5N1 polymerase complex. *Virus Res* 178:53–62. <https://doi.org/10.1016/j.virusres.2013.05.010>.
 46. de Jong MD, Simmons CP, Thanh TT, Hien VM, Smith GJ, Chau TN, Hoang DM, Chau NV, Khanh TH, Dong VC, Qui PT, Cam BV, Ha DQ, Guan Y, Peiris JS, Chinh NT, Hien TT, Farrar J. 2006. Fatal outcome of human influenza A (H5N1) is associated with high viral load and hypercytokinemia. *Nat Med* 12:1203–1207. <https://doi.org/10.1038/nm1477>.
 47. Puthavathana P, Auewarakul P, Charoenying PC, Sangsiriwut K, Pooruk P, Boonnak K, Khanyok R, Thawachsupa P, Kijphati R, Sawanpanyalert P. 2005. Molecular characterization of the complete genome of human influenza H5N1 virus isolates from Thailand. *J Gen Virol* 86:423–433. <https://doi.org/10.1099/vir.0.80368-0>.
 48. Subbarao EK, London W, Murphy BR. 1993. A single amino acid in the PB2 gene of influenza A virus is a determinant of host range. *J Virol* 67:1761–1764.
 49. Smith GJ, Naipospos TS, Nguyen TD, de Jong MD, Vijaykrishna D, Usman TB, Hassan SS, Nguyen TV, Dao TV, Bui NA, Leung YH, Cheung CL, Rayner JM, Zhang JX, Zhang LJ, Poon LL, Li KS, Nguyen VC, Hien TT, Farrar J, Webster RG, Chen H, Peiris JS, Guan Y. 2006. Evolution and adaptation of H5N1 influenza virus in avian and human hosts in Indonesia and Vietnam. *Virology* 350:258–268. <https://doi.org/10.1016/j.viro.2006.03.048>.
 50. Tao P, Ning Z, Hao X, Lin X, Zheng Q, Li S. 2019. Comparative analysis of whole-transcriptome RNA expression in MDCK cells infected with the H3N2 and H5N1 canine influenza viruses. *Front Cell Infect Microbiol* 9:76. <https://doi.org/10.3389/fcimb.2019.00076>.
 51. Simon PF, McCorrister S, Hu P, Chong P, Silaghi A, Westmacott G, Coombs KM, Kobasa D. 2015. Highly pathogenic H5N1 and novel H7N9 influenza A viruses induce more profound proteomic host responses than seasonal and pandemic H1N1 strains. *J Proteome Res* 14:4511–4523. <https://doi.org/10.1021/acs.jproteome.5b00196>.
 52. Martínez-Sobrido L, García-Sastre A. 2010. Generation of recombinant influenza virus from plasmid DNA. *J Vis Exp* 2010(42):2057. <https://doi.org/10.3791/2057>.
 53. Schickli JH, Flandorfer A, Nakaya T, Martínez-Sobrido L, García-Sastre A, Palese P. 2001. Plasmid-only rescue of influenza A virus vaccine candidates. *Philos Trans R Soc Lond B Biol Sci* 356:1965–1973. <https://doi.org/10.1098/rstb.2001.0979>.
 54. Du Y, Xin L, Shi Y, Zhang TH, Wu NC, Dai L, Gong D, Brar G, Shu S, Luo J, Reiley W, Tseng YW, Bai H, Wu TT, Wang J, Shu Y, Sun R. 2018. Genome-wide identification of interferon-sensitive mutations enables influenza vaccine design. *Science* 359:290–296. <https://doi.org/10.1126/science.aan8806>.
 55. Jorba N, Coloma R, Ortin J. 2009. Genetic trans-complementation establishes a new model for influenza virus RNA transcription and

- replication. *PLoS Pathog* 5:e1000462. <https://doi.org/10.1371/journal.ppat.1000462>.
56. Dobin A, Davis CA, Schlesinger F, Drenkow J, Zaleski C, Jha S, Batut P, Chaisson M, Gingeras TR. 2013. STAR: ultrafast universal RNA-seq aligner. *Bioinformatics* 29:15–21. <https://doi.org/10.1093/bioinformatics/bts635>.
57. Seaman WT, Andrews E, Couch M, Kojic EM, Cu-Uvin S, Palefsky J, Deal AM, Webster-Cyriaque J. 2010. Detection and quantitation of HPV in genital and oral tissues and fluids by real time PCR. *Virology* 7:194. <https://doi.org/10.1186/1743-422X-7-194>.
58. Yamato K, Fen J, Kobuchi H, Nasu Y, Yamada T, Nishihara T, Ikeda Y, Kizaki M, Yoshinouchi M. 2006. Induction of cell death in human papillomavirus 18-positive cervical cancer cells by E6 siRNA. *Cancer Gene Ther* 13:234–241. <https://doi.org/10.1038/sj.cgt.7700891>.
59. Soonthornvacharin S, Rodriguez-Frandsen A, Zhou Y, Galvez F, Huffmaster NJ, Tripathi S, Balasubramaniam VRMT, Inoue A, de Castro E, Moulton H, Stein DA, Sánchez-Aparicio MT, De Jesus PD, Nguyen Q, König R, Krogan NJ, García-Sastre A, Yoh SM, Chanda SK. 2017. Systems-based analysis of RIG-I-dependent signalling identifies KHSRP as an inhibitor of RIG-I receptor activation. *Nat Microbiol* 2:17022. <https://doi.org/10.1038/nmicrobiol.2017.22>.